ISSN: 0975-833X

Available online at http://www.journalcra.com

International Journal of Current Research
Vol. 5, Issue, 02, pp.240-247, February, 2013

INTERNATIONAL JOURNAL OF CURRENT RESEARCH

RESEARCH ARTICLE

Molecular structural, Spectroscopic (FT-IR, FT-Raman and UV–VIS) studies on the 3-(4-Fluorobenzoyl) Propionic acid by DFT calculations

Ramachandran S., and *Velraj, G.

Department of Physics, Periyar University, Salem 636 011, Tamil Nadu, India

ARTICLE INFO

Article History:
Received 15th November, 2012
Received in revised form
14th December, 2012
Accepted 20th January, 2013
Published online 14th February, 2013

Key words:

FT-IR;
FT-Raman;
DFT;
TD-DFT;
3-(4-fluorobenzoyl) propionic acid.

ABSTRACT

In the present study, the molecular structure, vibrational and electronic analyses of 3-(4-fluorobenzoyl) propionic acid (34FBPA, $C_{10}H_9FO_3$) were presented using experimental techniques (FT-IR, FT-Raman and UV-VIS) and density functional theory (DFT) employing B3LYP exchange correlation with the 6-31G(d)basis set. FT-IR and FT-Raman spectra were recorded in the regions of 4000–400 cm^{-1} and 4000–100 cm^{-1}, respectively. The UV–VIS absorption spectra of the compound that dissolved in ethanol and water solution were recorded in the range of 190–400 nm. The lower value in the highest occupied molecular orbital (HOMO) and lowest unoccupied orbital (LUMO) energy gap explains the eventual charge transfer interactions taking place within the molecule. The UV-VIS spectral analysis of 34FBPA has been calculated by theoretically in order to understand the electronic transitions of the compound, time-dependent DFT (TD-DFT) calculations on electronic absorption spectra in solvents (water and ethanol) were performed. The calculated frontier orbital energies (FMO), molecular electrostatic potential (MEP), absorption wavelengths (λ), oscillator strengths (f) and excitation energies (E) for solvent are also illustrated. Thermodynamic properties (heat capacity, entropy and enthalpy) of the title compound at different temperatures were calculated. Finally, the calculation results were compared with measured infrared and Raman spectra of the title compound which show good agreement with the observed spectra.

INTRODUCTION

The 3-(4-Flurobenzoyl) propionic acid (34FBPA) have the biological significance of these blocked dopamine-induced extracellular signal-regulated kinase 1/2 phosphorylation and it specifically affected mitogen-activated protein kinase kinase (MEK)1/2 activity in hippocampal HN33 (hippocampal neurons and N18TG2 neuroblastoma) cells (Kim *et al*., 2006). Moreover, 34FBPA was capable of direct interaction with MEK1/2 and inhibited its activity in vitro. Haloperidol, a dopamine D2 receptor blocker, is a classical neuroleptic drug that elicits extrapyramidal symptoms. Its metabolites include 3-(4-fluorobenzoyl) propionic acid (34FBPA) and 4-(4-chlorophenyl)-4-piperidinol (CPHP) (Seeman *et al*., 1998 and Jenner *et al*., 1980). The administration of 34FBPA to mice effected a repression of locomotor activity and induced catalepsy in a manner similar to that observed with haloperidol. 34FBPA may prove useful as an MEK inhibitor, as the targeted inhibition of specific signal transduction pathways has been hailed as a novel approach to the development of new drugs. Studies involving the conditional expression of a dominant-negative form of MEK have reported the occurrence of selective deficits in both hippocampal memory retention and long-term potentiation (Kelleher *et al*., 2004). The propionic acid exhibits antimycotic activity, its use is limited to foods in which the pH is fairly acidic, since it has virtually no activity at neutral or near neutral pH values (Molina *et al*., 2002). There exist many research reports on molecular structure of propionic acid derivatives (Al Azzam., 2010; Playne., 1985; Keshav *et al*., 2009; King *et al*., 1990 and Bilgin *et al* 2010). The DFT (density functional theory) and TD-DFT (time-dependent density functional theory) are of particular interest owing to give satisfactory results with experiment by costing low computational demands compared to the computational methods developed for the calculation of electronic structure and excitation energies of molecular systems (Nemykin *et al*., 2006 and Menconi *et al*., 2005).

Corresponding author: gvelraj@yahoo.co.uk

To the best of our knowledge, complete vibrational assignments based on FT-IR and FT-Raman using DFT calculations are not available in the literature for the title compound under investigation. Hence, the objectives of the present study were to evaluate the vibrational spectroscopic analysis and electronic properties of the 34FBPA using DFT (B3LYP/6-31G(d) calculations. This study is a part of a research program on the recovery of 34FBPA from dilute solutions using organic solvents. In addition, MEP and thermodynamic properties were obtained in the range of 100–700 K.

Experimental

The 34FBPA sample in solid state was purchased from Sigma-Aldrich Organics Company with a stated purity of 97% and it was used as such without further purification. The standard KBr technique with 1 mg of sample per 100 mg of KBr was used. The FT-IR spectrum of a molecule was recorded in the region 4000–400 cm^{-1} at a resolution of 2 cm^{-1} using BRUKER Tensor-27 FT-IR spectrometer. FT-Raman spectrum of the sample was recorded using 1064 nm line of Nd: YAG laser as the excitation wavelength in the region 4000–100 cm^{-1} on a Bruker RFS 100/S FT-Raman. The detector is a liquid nitrogen-cooled Ge detector. Five hundred scans were accumulated at a resolution of 4 cm^{-1} using a laser power of 100 mW. The ultraviolet (UV) absorption spectra of the compound dissolved in water and ethanol, were examined in the range of 190–400 nm using Perkin Elmer Lambda 25 UV–VIS Spectrophotometer.

COMPUTATIONAL DETAILS

The molecular structure optimisation of the title compound and corresponding fundamentals vibrational frequencies were calculated using the DFT with B3LYP/6-31G(d)basis set using GAUSSIAN 03 program package without any constraint on the geometry. The optimised geometrical parameters, true rotational constants, fundamental vibrational frequencies, IR intensity, Raman activity, electronic polarisability, atomic charges, dipole moment and other

thermodynamical parameters were calculated using the Gaussian 03 package (Frisch *et al*., 2000). By combining the results of the GAUSS-VIEW (Frisch *et al*., 2000) program with symmetry considerations, vibrational frequency assignments were made. The Raman activities have been converted to relative Raman intensities using the following relationship derived from the intensity theory of Raman scattering (Keresztury *et al*., 2002 and 1993).

$$I_i = \frac{f(\nu_o - \nu_i)^4 S_i}{\nu_i[1-\exp(-hc\nu_i / kT)]} \qquad (1)$$

where ν_o is the laser exciting wavenumber in cm^{-1} (in this article, we have used the excitation wavenumber ν_o = 9398.5 cm^{-1}, which corresponds to the wavelength of a Nd:YAG laser (1064nm)), ν_i is the vibrational wavenumber of the *i*th normal mode (cm^{-1}) and Si is the Raman scattering activity of the normal mode ν_i . *f* (is a constant equal to 10^{-12}) is a suitably chosen common normalisation factor for all peak intensities. *h*, *k*, *c* and *T* are Planck and Boltzmann constants, speed of light, temperature in Kelvin, respectively. Next, the spectra were analysed in terms of the potential energy distribution (PED) contributions by using the *vibrational energy distribution analysis* (VEDA) program (Jamroz, 2004).

a molecule is defined in terms of the interaction energy between the electrical charge generated from the molecule's electrons and nuclei and a positive test charge (a proton) located at *r*. The values of *V*(*r*) were calculated as described previously using the following equation (Politzer *et al*., 2002).

$$V(r) = \sum \frac{Z_A}{|R_A - r|} - \int \frac{\rho(r')}{|r' - r| d^3 r'} \qquad (2)$$

where Z_A is the charge of nucleus *A*, located at R_A, $\rho(r')$ is the electronic density function of the molecule and r' is the dummy integration variable. In addition, the thermo dynamical study was performed at the B3LYP/6-31G(d)level.

RESULTS AND DISCUSSION

Molecular Geometry

The structure and the scheme of numbering the atoms of 34FBPA are shown in Fig. 1. The optimised structural parameters of 34FBPA are calculated at the B3LYP level of theory using 6-31G(d) basis set. The geometry of the molecules under investigation is considered to possess C_S point group symmetry and the corresponding global minimum energy was calculated to be *E* = –712.228094845 a.u.
The calculated geometric parameters in DFT methods with

Table 1. Optimised geometric data for 34FBPA using B3LYP/6-31G(d)

Bond length	Exp.[a] (Å)	Value (Å)	Bond angle	Exp.[a] (°)	Value (°)
C_1–C_2	1.493	1.508	C_2–C_1–O_4	113.8	126.2
C_1–O_4	1.243	1.206	C_2–C_1–O_5	122.3	111.3
C_1–O_5	1.291	1.355	O_4–C_1–O_5	122.5	122.3
C_2–C_3	1.517	1.523	C_1–C_2–C_3	115.1	112.4
C_2–H_{15}	–	1.093	C_1–C_2–H_{15}	–	108.2
C_2–H_{16}	–	1.093	C_1–C_2–H_{16}	–	108.2
C_3–C_6	1.494	1.522	C_3–C_2–H_{15}	–	111.2
C_3–H_{17}	–	1.094	C_3–C_2–H_{16}	–	111.2
C_3–H_{18}	–	1.094	H_{15}–C_2–H_{16}	–	104.8
O_5–H_{19}	1.13	0.969	C_2–C_3–C_6	113.3	112.7
C_6–C_7	–	1.498	C_2–C_3–H_{17}	–	110.2
C_6–O_{13}	1.226	1.217	C_2–C_3–H_{18}	–	110.2
C_7–C_8	1.401	1.403	C_6–C_3–H_{17}	–	109.0
C_7–C_{12}	1.405	1.401	C_6–C_3–H_{18}	–	109.0
C_8–C_9	1.379	1.387	H_{17}–C_3–H_{18}	–	105.1
C_8–H_{20}	–	1.082	C_1–O_5–H_{19}	114.0	107.2
C_9–C_{10}	1.397	1.388	C_3–C_6–C_7	124.8	118.4
C_9–H_{21}	–	1.082	C_3–C_6–O_{13}	–	120.9
C_{10}–C_{11}	1.372	1.386	C_7–C_6–O_{13}	–	120.6
C_{10}–F_{14}	–	1.351	C_6–C_7–C_8	–	118.1
C_{11}–C_{12}	1.393	1.391	C_6–C_7–C_{12}	–	122.8
C_{11}–H_{22}	–	1.082	C_8–C_7–C_{12}	119.1	118.9
C_{12}–H_{23}	–	1.082	C_7–C_8–C_9	118.6	120.9
			C_7–C_8–H_{20}	–	118.4
			C_9–C_8–H_{20}	–	120.6
			C_8–C_9–C_{10}	121.1	118.3
			C_8–C_9–H_{21}	–	121.8
			C_{10}–C_9–H_{21}	–	119.7
			C_9–C_{10}–C_{11}	121.8	122.5
			C_9–C_{10}–F_{14}	–	118.7
			C_{11}–C_{10}–F_{14}	–	118.7
			C_{10}–C_{11}–C_{12}	117.2	118.3
			C_{10}–C_{11}–H_{22}	–	119.8
			C_{12}–C_{11}–H_{22}	–	121.7
			C_7–C_{12}–C_{11}	122.2	120.8
			C_7–C_{12}–H_{23}	–	120.6
			C_{11}–C_{12}–H_{23}	–	118.5

The electronic properties, such as HOMO–LUMO energies, absorption wavelengths and oscillator strengths, were calculated using the B3LYP method of TD-DFT (Runge *et al*., 1984; Petersilka *et al*., 1996; Bauernschmitt *et al*., 1996 and Jamorski *et al*., 1996) based on the optimised structure. To study the reactive sites of the title compound, MEP was evaluated using the B3LYP/6-31G(d)method. MEP, *V*(*r*), at a given point *r*(*x*, *y*, *z*) in the vicinity of

B3LYP/6-31G(d) levels for 34FBPA were compared with the experimentally available X-Ray diffraction data (Okabe *et al*., 1998) in Table 1. As can be seen, there was agreement between experimental and the calculated geometric parameters. Some deviations from the experimentally observed values can be attributed to hydrogen bonds in the solid state. The biggest deviation between the calculated and experimental bond length and bond angles are

noted for the C_1–O_5, O_5–H_{19} and C_2–C_1–O_4, C_2–C_1–O_5, C_1–O_5–H_{19}, C_3–C_6–C_7, respectively. The calculated bond lengths and angles represent a good approximation in spite of these differences; and they became the basis for calculating other parameters, such as vibrational frequencies, electronic properties, MEP and thermodynamic properties, as described below.

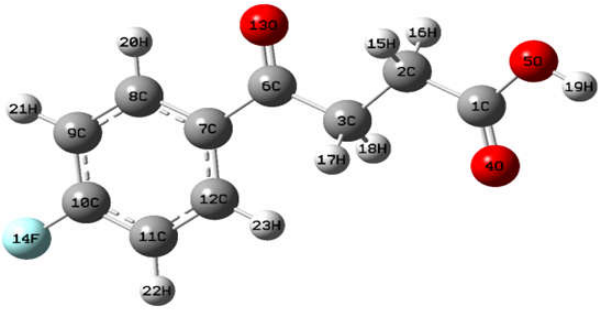

Fig. 1. Optimisation structure and atom number of numbering scheme of 34FBPA

Analysis of Spectra and Theoretical Simulations

The 63 fundamental modes of vibrations of the title compound are distributed into the irreducible representation under C_S symmetry as $\Gamma 3N\text{-}6_{vib} = 43A' + 20A''$. The vibrations of the A' species are in-plane and those of the A'' species are out-of-plane. All the frequencies are assigned in terms of fundamental, overtone and combination bands. All vibrations were active in both Raman scattering and infrared absorption. In Raman spectrum, the A' vibrations give rise to polarised bands while the A'' ones to depolarised bands. For visual comparison, the observed and calculated (simulated) spectra of 34FBPA are shown in Figs. 2 and 3 on a common frequency scale. Comparison between the calculated and observed vibrational spectra helps us to understand the observed spectral features. The graphic correlations between the experimental and calculated frequencies obtained are depicted in Fig. 4.

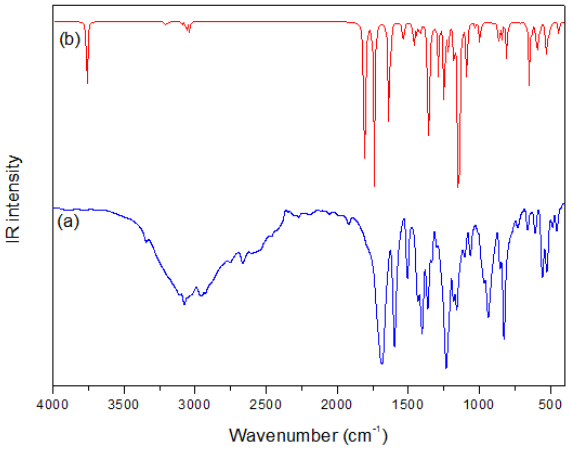

Fig. 2. FT-IR spectrum: (a) observed; (b) 6-31G(d)

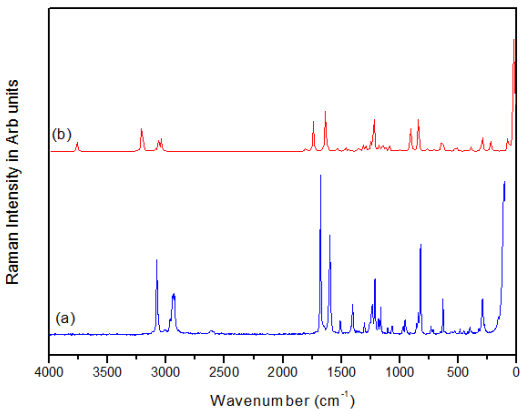

Fig. 3. FT-Raman spectrum: (a) observed; (b) 6-31G(d)

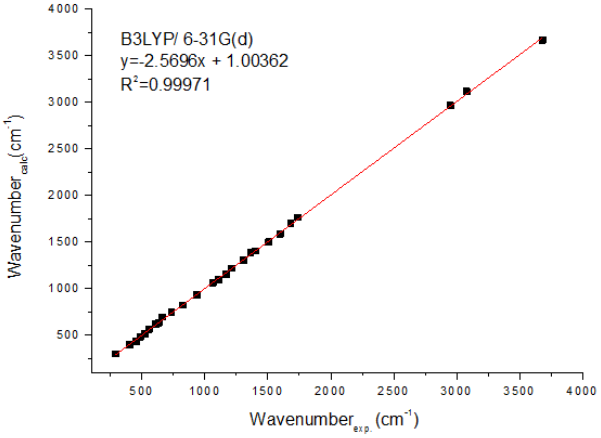

Fig. 4. Correlation graph between the experimental and calculated frequencieobtained by B3LYP/ 6-31G(d)methods

C–H Vibrations

The aromatic C–H stretching vibrations (Sridevi *et al*., 2012) are observed in the region of 3100–2800 cm^{-1}. Accordingly, in the title compound, antisymmetric stretching vibrations of C–H were observed at 3076 cm^{-1} and 3079 cm^{-1} in the FT-IR and FT-Raman spectrum, whereas in the symmetric stretching vibrations is observed in 2948 cm^{-1} in the FT-Raman, respectively. The in-plane bending and out-of-plane bending vibrations of the aromatic C–H group have also been identified for the title compound and they are presented in Table 2. It is known that the C–H in-plane bending vibrations (Sridevi *et al*., 2012) are observed in the region of 1025–1280 cm^{-1}. The FT-Raman vibrations are assigned to C–H in-plane bending vibrations at 1108 cm^{-1}. In the FT-IR and FT-Raman vibrations, the C–H out-of-plane bending is observed at 937 cm^{-1} and 955 cm^{-1}, respectively.

Table 2. The observed and calculated frequencies using B3LYP/6-31G (d)for 34FBPA

Species C_S	Experimental wavenumbers (cm^{-1})[a]		Calculated wavenumbers (B3LYP)(cm^{-1})			Vibrational assignments (PED)[b]
	FT–IR	FT–Raman	Scaled value	IR Intensity	Raman Intensity	
A'	3681VW	–	3666	74.50	44.40	υ_s O–H (100)
	3344M	–				Overtone + combination
A'		–	3130	3.59	118.86	υ_s C–H (96)
A'	–	–	3127	1.62	8.61	υ_{as} C–H (95)
A'	–	–	3115	0.04	37.82	υ_{as}C–H (77)
A'	3076VS	3079W	3113	3.24	9.79	υ_{as} C–H (76)
A''	–	–	3015	4.36	8.80	υ_{as} C–H (69)
A''	–	–	2988	1.85	28.53	υ_{as} C–H (71)
A'	–	–	2984	9.59	37.88	υ_s C–H (64)
A'	–	2948W	2963	13.39	61.80	υ_s C–H (48)
	1810WV					Overtone + combination

A'	1738M	–	1761	265.51	18.84	υ C=O (54) + β O–H (21)
A'	1678VS	1683VS	1697	198.69	137.40	υ C=O (61)
A'	–	–	1596	147.90	241.63	υ C–C (66) + υ C–F (18)
A'	1597VS	1608M	1584	31.02	31.319	υ C–C (56) + υ C=O (21)
A'	1506VS	–	1497	38.48	18.82	υ C–C (36) + β C–H (20)
A'	–	–	1429	9.14	9.46	δ C–H_2 (66)
A'	–	–	1422	25.55	12.22	δ C–H_2 (61)
A'	1403VS	1402VW	1402	15.78	9.19	υ C–C (28) + β C–H (22)
A'	1363VS	–	1380	21.39	30.36	ω C–H_2 (32)
A'	–	–	1322	234.65	18.83	ω C–H_2 (33)
A'	–	1307VW	1307	7.45	5.61	υ C–C (71)
A'	–	–	1287	2.56	3.56	β C–H (52)
A'	–	–	1277	0.34	27.55	t C–H_2 (87)
A'	–	–	1258	63.41	20.64	ω C–H_2 (36) + β O–H (31)
A'	1235VS	1214W	1217	108.25	48.06	υ C–F (48) + β C–H (18)
A'	–	–	1191	37.48	184.26	ω C–H_2 (34)
A'	–	1167VW	1149	0.20	0.14	t C–H_2 (83)
A'	–	–	1147	57.72	42.25	β C–H (64)
A'	–	–	1116	376.75	43.31	ω C–H_2 (36) + β O–H (27)
A'	–	1108VW	1094	7.74	17.44	β C–H (54)
A'	1063S	1066VW	1064	67.51	24.03	ω C–H_2 (43) + υ C–C (28)
A''	–	–	1007	1.35	4.81	ρ C–H (37)
A'	–	–	1003	4.68	0.88	β C–H (58)
A'	–	–	971	36.41	8.34	υ C–C (47) + ω C–H_2 (36)
A''	–	–	970	0.13	0.07	γ C–H (71)
A''	937VS	955VW	934	0.26	0.05	γ C–H (73)
A'	–	–	884	2.46	138.72	ω C–H_2 (38) + β O–H (26)
A''	–	–	842	35.21	0.64	γ C–H (57)
A'	825VS	824M	821	20.62	167.46	Ring deformation
A''	–	–	811	0.10	0.13	γ C–H (74)
A''	–	–	788	52.37	1.21	ρ C–H (48)
A'	–	736VW	748	0.24	15.77	υ_s C–H_2 (53) + β O–H (29)
A''	660W	–	694	2.217	6.35	Ring deformation
A''	–	634W	633	77.72	3.51	γ O–H (79)
A'	–	–	629	1.08	66.75	β C–C (74)
A'	608W	–	613	8.76	24.79	β O–H (48) + δ C–O (20)
A'	–	–	580	57.52	7.06	Ring deformation
A''	556S	–	561	19.20	2.46	ρ C–H_2(41)
A'	525S	–	516	38.32	7.88	β O–H(38)
A''	–	–	501	27.73	24.42	γ O–H (51) + ρ C–H_2 (29)
A''	486W	488VW	481	4.80	6.47	ρ C–H_2 (36)
A'	454W	–	428	15.18	4.45	Ring deformation
A''	–	403VW	401	0.02	0.14	γ C–H_2 (66)
A'	–	–	382	1.41	24.91	β C–F (37)
A'	–	292VW	296	1.81	40.61	β C=O(42)
A''	–	–	284	0.41	62.25	γ C=O (33)
A'	–	–	218	0.75	77.10	τ C–C–C–C (42)
A'	–	–	187	9.53	2.48	τ C–C–O–H (64)
A''	–	–	110	1.18	1.66	ρ C–H_2 (73)
A''	–	–	80	0.00	60.77	ρ C–H_2 (67)
A'	–	–	68	1.02	25.97	β C–O (41) + β C–H_2 (23)
A''	–	–	57	3.16	13.83	ρ C–H_2 (57)
A''	–	–	27	0.01	720.05	γ C–H_2 (39)
A''	–	–	13	3.35	80.81	ρ C–H_2 (61) + γ C–O (18)

[a]vs– a very strong; s–strong; m–medium strong; w–weak; vw–very weak

[b]υ– stretching; υ_s–symmetric stretching; υ_{as}– antisymmetric stretching; γ– out of plane bending; β– in plane bending; τ– torsion; ρ– rocking; δ– scissoring; ω –wagging; t–twisting.

C–C Vibrations

The aromatic ring stretching vibrations is expected within the region of 1650–1200 cm^{-1} (Surisseau *et al*., 1994 and Barnes *et al*., 1985). Most of the ring modes are altered by the substitution to the aromatic ring. Generally, the C–C stretching vibrations in aromatic compounds form the strong bands. In the present study, the bands of different intensities were observed at 1597, 1506 and 1403 cm^{-1} in FT-IR and 1608, 1402 and 1307cm^{-1} in FT-Raman have been assigned to C–C stretching vibrations. The theoretically calculated values at 1584, 1497, 1402, 1380 and 1307 cm^{-1} by B3LYP/6-31G(d) method shows agreement with experimental data.

O–H Vibrations

The high frequency region above 3000 cm^{-1} is the characteristic region for the steady identification of C–H, O–H and N–H stretching vibrations (Silverstein *et al*., 1981). The carboxylic acid O–H stretching band is weak in the Raman spectrum, so IR data are generally used. The O–H stretching is characterised by a very broad band appearing nearly about 3400–3600 cm^{-1}. The O–H group gives rise to three vibrations: stretching, in-plane bending and out-of-plane bending vibrations. The O–H stretching vibration of 34FBPA is observed at 3681 cm^{-1} in the FT-IR spectrum. The O–H in-plane bending is observed in 525 and 608 cm^{-1}. The O–H group vibrations are likely to be the most sensitive to the environment, so they show pronounced shifts in the spectra of the hydrogen-bonded species (Michalska *et al*., 1996).

C=O and C–F Vibrations

The band due to C=O stretching vibration is observed in the region of 1850–1550 cm^{-1} (Socrates 2001). In the present work, the bands observed at 1738 and 1678 cm^{-1} in FT-IR spectrum and 1683 cm^{-1} in Raman are assigned to C=O stretching mode of vibrations, respectively. The (C–F) stretching modes originate from medium

intensity infrared absorptions at 1235 cm^{-1}, with counterparts at 1214 cm^{-1} in the Raman spectrum. These values are in accordance with the literature values (Silverstein *et al*., 2005).

UV–Vis Study and Electronic Properties

Electronic transitions are usually classified according to the orbitals engaged or to specific parts of the molecule involved. Common types of electronic transitions in organic compounds are π (donor), $-\pi*$ (acceptor) and $n-\pi*$ (Dhas *et al*., 2010 and Cetin *et al* 2011). The inner is called weak transition, whereas the latter is termed as the strong transition. In order to understand the electronic transitions of the title compounds studied in this paper, theoretical calculations on electronic absorption spectra are performed in vacuum by B3LYP/6-31G(d)method (Bauernschmitt *et al*., 1996; Furche *et al*., 2002 and Yildirim *et al*., 2011). The simulated UV spectra of studied molecule are given in Fig. 5.

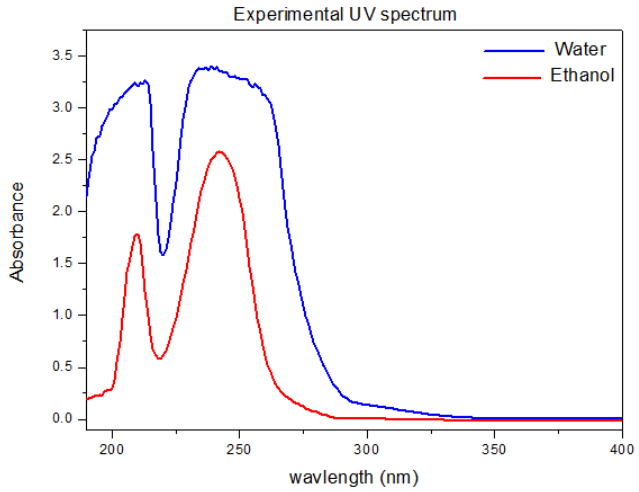

Fig. 5. Experimental UV-VIS spectra of 34FBPA in water and ethanol solution

associated within the framework of self-consistent field (SCF) molecular orbital (MO) theory. The ionisation energy and electron affinity can be expressed through HOMO and LUMO orbital energies as $I = -E_{HOMO}$ and $A = -E_{LUMO}$. The hardness corresponds to the gap between the HOMO and LUMO orbital energies. The larger the HOMO–LUMO energy gaps the harder the molecule (Udhayakala *et al*., 2011). The global hardness is $\eta = ½ (E_{LUMO} - E_{HOMO})$. The hardness has been associated with the stability of chemical system. The electron affinity can be used in combination with ionisation energy to give electronic chemical potential, $\mu = ½ (E_{HOMO} + E_{LUMO})$.

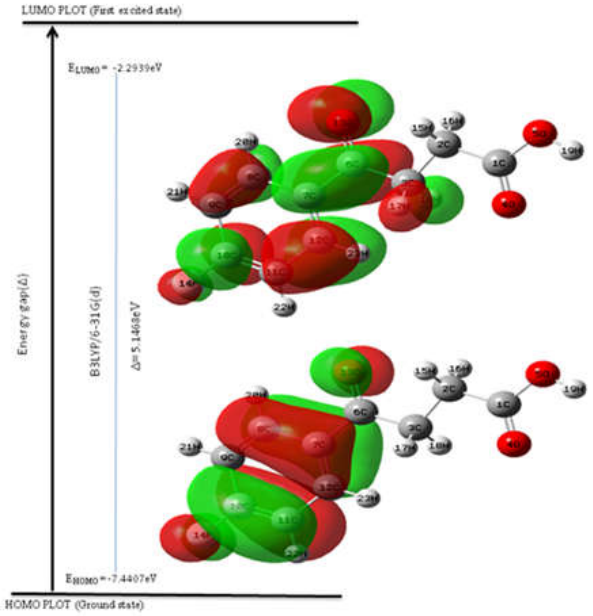

Fig. 6. Molecular orbital surfaces for the HOMO and LUMO of 34FBPA

The global electrophilicity index, $\omega = \mu^2/2\eta$, is also calculated and listed in Table 4.

Table 3. Experimental and calculated absorption wavelength λ (nm), excitation energies *E* (eV) and oscillator strengths (*f*) of 34FBPA calculated by the B3LYP method using 6-31G(d)basis set

Assignments	Experimental						TD–DFT (B3LYP)/6–31 G(d)					
	Ethanol			Water			Ethanol			Water		
	λ (nm)	*E* (eV)	Abs.	λ (nm)	*E* (eV)	Abs.	λ (nm)	*E* (eV)	*f*(a.u.)	λ (nm)	*E* (eV)	*f*(a.u)
$\pi \rightarrow \pi^*$	241.95	5.122	2.583	238.99	5.103	3.400	258.33	4.780	0.0857	258.26	4.782	0.0836
$\pi \rightarrow \pi^*$	210.01	5.881	1.780	213.01	5.798	3.264	217.43	5.680	1.1471	217.31	5.683	0.1435

The experimental peaks together with the calculated excitation energies, oscillator strength (*f*), absorption wavelength (λ) and spectral assignments are given in Table 3. The frontier molecular orbital (FMO) plays an important role in the electrical and optical properties (Fleming, 1976). The frontier orbital gap helps to characterise the chemical reactivity and kinetic stability of the molecule. A molecule with a small frontier orbital gap is more polarisable, generally associated with a high chemical reactivity, low kinetic stability and is termed as soft molecule. The wave function indicates that the electronic absorption corresponds to the transition from the ground to the first excited state and is mainly described by one-electron excitation from the highest occupied molecular orbital (HOMO) to the lowest unoccupied orbital (LUMO). The Fig. 6 shows the distributions and energy level of the HOMO and LUMO orbital computed at the B3LYP/6-31G(d) level for our 34FBPA. The value of the energy separation between the HOMO and LUMO is 5.1468 eV. This low value makes it more reactive and less stable. The atomic orbital compositions of the frontier molecule orbital are

Table 4. The atomic orbital compositions of the frontier molecular orbital for 34FBPA

Molecular Energy	B3LYP/6–31 G(d)
E_{HOMO}	–7.4407
E_{LUMO}	–2.2939
Energy gap(Δ)	5.1468
Ionisation Potential (I)	7.4407
Electron affinity(A)	2.2939
Global Hardness (η)	2.5734
Chemical potential (μ)	–4.8673
Global Electrophilicity (ω)	4.6029

Molecular Electrostatic Potential

MEP is related to the electronic density. It is a very useful descriptor in understanding sites for electrophilic attacks and nucleophilic reactions as well as hydrogen bonding interactions (Luque *et al*., 2000). The importance of MEP lies in the fact that it simultaneously

displays molecular size, shape as well as positive, negative and neutral electrostatic potential regions in terms of colour grading (Fig. 7). It is helpful in research of molecular structure with its physiochemical property relationship (Murray *et al*., 1996 and Scrocco *et al*., 1978). The different values of the electrostatic potential at the surface are represented by different colours. Potential increases in the order red < orange < yellow < green < blue. The colour code of these maps is in the range between −4.210 kcal/mol (red) and +4.210 kcal/mol (blue) in the compound, where blue indicates the strongest attraction and red indicates the strongest repulsion. The regions of negative $V(r)$ are usually associated with the lone pair of electronegative atoms. As can be seen from the MEP map of the title molecule, while regions having the negative potential are over the electronegative atom (oxygen atom), the regions having the positive potential are over the hydrogen atoms. From these results, we can say that the hydrogen atoms indicate the strongest attraction and oxygen atom indicates the strongest repulsion.

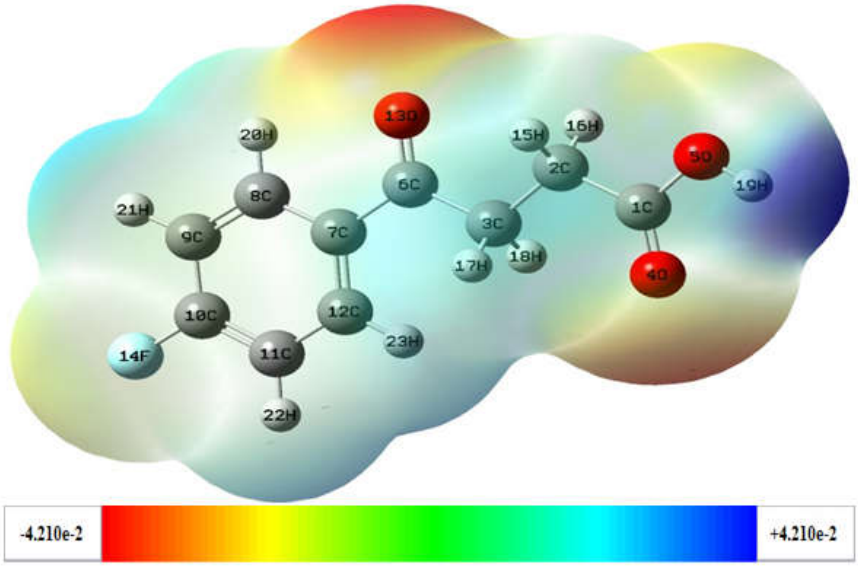

Fig. 7. Molecular electrostatic potentials of 34FBPA (B3LYP/6-31G(d), 0.004 a.u., energy values –4.210 to +4.210 kcal/mol); colour coding: red (very negative), orange (negative), yellow (slightly negative), green (neutral), turquoise (slightly positive), light blue (positive), dark blue (very positive).

Table 5. The calculated thermodynamic parameters of 34FBPA employing B3LYP/6-31G(d) methods

Thermodynamic parameters (298K)	B3LYP/6–31G(d)
SCF energy (a.u.)	–712.228094845
Total energy (thermal), E_{total} (kcal mol^{-1})	116.350
Heat capacity at const. volume, C_v (cal mol^{-1}K^{-1})	46.854
Entropy, S (cal mol^{-1}K^{-1})	119.328
Vibrational energy, E_{vib} (kcal mol^{-1})	114.572
Zero–point vibrational energy, E_0 (kcal mol^{-1})	108.26584
Rotational constants (GHz)	
A	2.10731
B	0.24802
C	0.22250
Dipole moment (Debye)	
μ_x	0.6277
μ_y	–0.6037
μ_z	–0.3482
μ_{total}	0.9379

Thermodynamical Properties

Several thermodynamic parameters performed by B3LYP with 6-31G(d) level of theory are given in Table 5. Scale factors were recommended (Foresman *et al*., 1996) for an accurate prediction in determining the zero-point vibration energies. The total energies and changes in the total entropy of the compounds at room temperature were presented. Table 5 indicates several thermodynamic parameters of the molecule without experimental determinations. The energy 34FBPA has been calculated as –712.2280a.u. The thermodynamic data provide helpful information for further study on the title compound. The dipole moment and its principal inertial axes strongly depend upon the molecular conformation. Dipole moment reflects the molecular charge distribution and is given as a vector in three dimensions. Therefore, it can be used as a descriptor to depict the charge movement across the molecule.

Table 6. Thermodynamic properties at different temperatures at the B3LYP/ 6-31G(d)level of 34FBPA

T(K)	$C^0_{p,m}$ (cal mol^{-1}K^{-1})	S^0_m (cal mol^{-1}K^{-1})	H^0_m (Kcal mol^{-1})
100	14.932	17.879	109.135
200	27.326	31.880	111.226
298.15	40.893	45.312	114.572
300	41.147	45.566	114.648
400	54.138	59.223	119.426
500	65.083	72.520	125.406
600	73.913	85.197	132.372
700	81.016	97.143	140.131

Diresction of the dipole moment vector in a molecule depends on the centres of positive and negative charges. Dipole moments are strictly determined for neutral molecules. For charged systems, its value depends on the choice of origin and molecular orientation. On the basis of vibrational analysis at B3LYP/6-31G(d) level, the standard statistical thermodynamic functions: heat capacity ($C^0_{p,m}$), entropy (S^0_m) and enthalpy changes (H^0_m) for the title compound were obtained from the theoretical harmonic frequencies and listed in Table 6. Therefore, it can be observed that these thermodynamic functions are increasing with temperature ranging from 100 K to 700 K due to the fact that the molecular vibrational intensities increase with temperature (Ott *et al*., 2000 and Sajan *et al*., 2011). The correlation equations among heat capacities, entropies, enthalpy changes and temperatures were fitted by quadratic, linear and quadratic formula and the corresponding fitting factors (R^2) for these thermodynamic properties are 0.99957, 0.99997 and 0.99971. The corresponding fitting equations are as follows and the correlation graphics of those are shown in Figs. 8–10.

$$C^0_{p,m} = -1.83066 + 0.1642T - 6.4227\times10^{-5}T^2 \quad (R^2 = 0.99957)$$

$$S^0_m = 3.16547 + 0.14747T - 1.84592\times10^{-5}T^2 \quad (R^2 = 0.99997)$$

$$\Delta H^0_m = 107.84214 + 0.00567T + 1.89583\times10^{-6}T^2 \quad (R^2 = 0.99971)$$

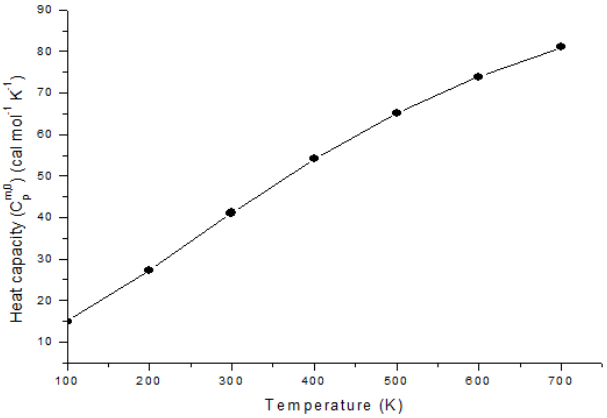

Fig. 8. Correlation graph of heat capacity and temperature for 34FBPA molecule

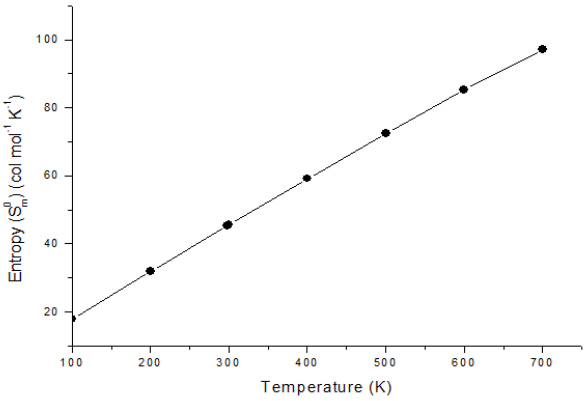

Fig. 9. Correlation graph of entropy and temperature for 34FBPA molecule.

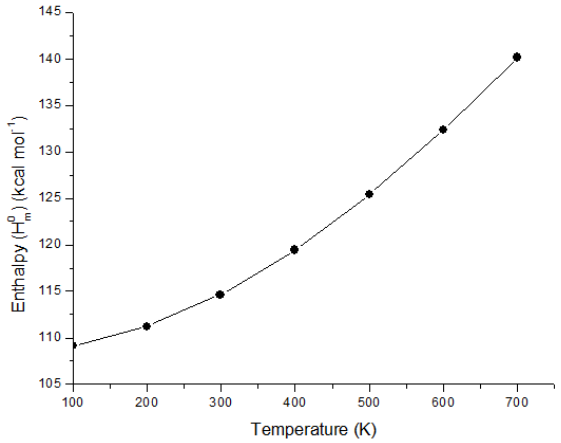

Figure 10. Correlation graph of enthalpy and temperature for 34FBPA molecule

All the thermodynamic data are supportive for the further study on the 34FBPA. They can be used to compute other thermodynamic energies according to the relationships of thermodynamic functions and estimate directions of chemical reactions according to the second law of thermodynamics in thermo chemical field (Zhang *et al*., 2011). Note: All thermodynamic calculations were done in gas phase and they could not be used in solution.

Conclusion

In this paper, the compound 34FBPA was experimentally characterised by means of FT-IR, FT-Raman and UV–vis spectroscopic techniques. The calculated geometrical parameters and vibrational frequencies obtained with DFT calculations B3LYP/6-31G(d)method are in good agreement with the experimental values obtained for the investigated molecule. To evaluate the electronic transitions and charge distribution, the UV spectra of the title compound were recorded in ethanol and water solutions. The obtained absorption maxima at 241nm (in ethanol) and 242 nm (in water) were predicted possibly due to HOMO → LUMO transition and assigned as $\pi \rightarrow \pi^*$. The TD-DFT calculations starting from optimised geometry were carried out in water and ethanol solution phase to calculate excitation energies. The TD-DFT method predicted the maximum absorption peak at 258 nm in ethanol with an oscillator strength $f = 0.0857$ a.u and coincide with experimentally obtained value. In addition, the MEP and the changes of thermodynamic properties were obtained.

Acknowledgement

One of the authors, S. Ramachandran gratefully acknowledges Periyar University for providing financial assistance through University Research Fellowship (URF).

REFERENCES

Al Azzam, K. M., Bahruddin, S., Hashim, N. H., Rahim, A. A., and Talib, K. M. 2010. Khairuddin Mohd Talib, Determination of propionates and propionic acid in bakery products using gas chromatography. *Int. Food Res. J.* 17: 1107–1112.

Barnes, A. J., Majid, M. A., Stuckey, M. A., Gregory, P., and Stead, C. V. 1985. The resonance Raman spectra of Orange II and Para Red: molecular structure and vibrational assignment. *Spectrochim. Acta A*. 41: 629–635.

Bauernschmitt, R., and Ahlrichs, R. *Chem. 1996.* Treatment of electronic excitations within the adiabatic approximation of time dependent density functional theory. *Phys. Lett*. 256: 454–464.

Bilgin, M., and Birman, I. 2010. Separation of propionic acid by diethyl carbonate or diethyl malonate or diethyl fumarate and the synergistic effect of phosphorus compounds and amines. *Fluid Phase Equilib*. 292: 13–19.

Cetin, S., Yildirim, G., Parlak, C., Akdogan, M., and Terzioglu, C. 2011. Experimental and theoretical studies on the identification of p-biphenyloxycarbonylphenyl acrylate. *Spectrochim. Acta A*. 79: 1024–1033.

Dhas, D. A., Joe, I. H., Roy, S. D. D., and Freeda, T. H. 2010. DFT computations and spectroscopic analysis of a pesticide: Chlorothalonil. *Spectrochim. Acta A*. 77: 36–44.

Fleming, I. 1976. Frontier Orbitals and Organic Chemical Reactions, Wiley, London.

Foresman, J. B., and Frisch, A.1996. Exploring Chemistry with Electronic Structure Methods, 2nd ed., Gaussian Inc., Pittsburgh, PA, USA.

Frisch, A., Nielson, A. B., and Holder, A. J. 2000. GAUSSVIEW User Manual, Gaussian Inc., Pittsburgh, PA.

Frisch, M. J., Trucks, G. W., Schlegel, H. B., Scuseria, G. E., Robb, M. A., Cheeseman, J. R., Montgometry Jr, J. A., Vreven, T., Kudin, K. N., Burant, J. C., Milliam, J. M., Iyengar, S. S., Jomasi, J., Barone, V., Mennucci, B., Cossi, M., Scalmani, G., Rega, N., Petersson, G. A., Nakatsuji, H., Hada, M., Ehara, M., Toyota, K., Fukuda, R., Hasegawa, J., Ishida, M., Nakajima, T., Honda, Y., Kitao, O., Nakai, H., Klene, M., Li, X., Knox, J. E., Hratchian, H. P., Cross, J. B., Adamo, C., Jaramillo, J., Gomperts, R., Stratmann, R. E., Yazyev, O., Austin, A. J., Cammi, R., Pomelli, C., Ochterski, J. W., Ayala, P. Y., Morokuma, K., Voth, G. A., Salvador, P., Dannenberg, J. J., Zakrzewski, V. G., Dapprich, S., Daniels, A. D., Strain, M. C., Farkas, O., Malick, D. K., Rabuck, A. D., Raghavachari, K., Foresamn, J. B., Ortiz, J. V., Cui, A., Baboul, A. G., Clifford, S., Cioslowski, J., Stefanov, B. B., Liu, G., Lashenko, A., Piskorz, P., Komaromi, I., Martin, R. I., Fox, D. J., Keith, T., Al-Lham, M. A., Peng, C. Y., Nanayakkara, A., Challacombe, M., Gill, P. M. W., Johnson, B., Chen, W., Wong,

M. W., Gonzalez, C., and Pople, J. A. 2003. Gaussian 03, Revision A.1, Gaussian, Inc., Pittsburgh, PA.

Furche, F., and Ahlrichs, R. J., 2002. Adiabatic time-dependent density functional methods for excited state properties. J. Chem. Phys. 117: 7433–7447.

Jamorski, C., Casida, M. E., and Salahub, D. R. 1996. Dynamic polarizabilities and excitation spectra from a molecular implementation of time-dependent density-functional response theory: N_2 as a case study *J. Chem. Phys*. 104: 5134–5147.

Jamroz, M. H. 2004. Vibrational Energy Distribution Analysis, VEDA 4, Warsaw.

Jenner, P., Marsden, C. D., and Thanki, C. M. *Br.* 1980. Behavioural changes induced by N,N-dimethyltryptamine in rodents. *J. Pharmacol*. 69: 69–80.

Kelleher, R. J., Govindarajan, A., Jung, H. Y., Kang, H., and Tonegawa, S. 2004. Translational Control by MAPK Signaling in Long-Term Synaptic Plasticity and Memory**.** *Cell*, 116 467–479.

Keresztury, G., Chalmers, J. M., and P. R. Griffith (Eds.). 2002. Raman Spectroscopy: Theory, In Hand book of Vibrational Spectroscopy, vol. 1, John Wiley & Sons Ltd., New York.

Keresztury, G., Holly, S., Varga, J., Besenyei, G., Wang, A. Y., and Durig, J. R. 1993. Vibrational spectra of monothiocarbamates. II. IR and Raman spectra, structure, and ab initio force field of S-methyl-N,N-dimethylthiocarbamate. *Spectrochim. Acta A*. 49: 2007–2026.

Keshav, A., Wasewar, K. L., Chand, S., and Uslu, H. 2009. Effect of binary extractants and modifier–diluents systems on equilbria of propionic acid extraction. *Fluid Phase Equilib*. 275: 21–26.

Kim, H. S., Song, M., Yumkham, S., Choi, J. H., Lee, T., Kwon, J., Lee, S. J., Kim, J., Lee, K. W., Han, P. L., Shin, S. W., Baik, J. H., Kim, Y. S., Ryu S. H., and Suh, P. G. 2006. Identification of a new functional target of haloperidol metabolite: implications for a receptor-independent role of 3-(4-fluorobenzoyl) propionic acid. *J. Neurochem*. 99: 458–469.

King, C. J., and Tamada, J. A. 1990. Extraction of carboxylic acids with amine extractants chemical interactions and interpretation of data. *Ind. Eng. Chem. Res*. 29: 1327–1333.

Luque, F. J., Lopez, J. M., and Orozco, M. 2000. Perspective on Electrostatic interactions of a solute with a continuum. A direct utilization of ab initio molecular potentials for the prevision of solvent effects. *Theor. Chem. Acc*. 103: 343–345.

Menconi, G., Kaltsoyannis, N. 2005. Time dependent DFT study of the electronic transition energies of RuO(4)and OsO4.Chemical Physics Letters. 415: 64-68

Michalska, D., Bienko, D. C., Abkowicz-Bienko, A. J., Latajka, Z. 1996. Density Functional, Hartree−Fock, and MP2 Studies on the Vibrational Spectrum of Phenol. *J. Phys. Chem*. 100: 17786–17790.

Molina, M., and Giannuzzi, L. 2002. Modelling of aflatoxin production by Aspergillus parasiticus in a solid medium at different temperatures, pH and propionic acid concentrations**.** *Food Res. Int*. 35: 585–594.

Murray, J. S., and Sen, K. 1996. Molecular Electrostatic Potentials, Concepts and Applications, Elsevier, Amsterdam.

Nemykin, V. N., Olsen, J. G., Perera, E., and Basu, P. 2006. Synthesis, Molecular and Electronic Structure, and TDDFT and TDDFT-PCM Study of the Solvatochromic Properties of $(Me_2Pipdt)Mo(CO)_4$Complex(Me_2Pipdt= *N*,*N*ʿ-Dimethylpiperazine-2,3-dithione). *Inorg. Chem*. 45: 3557–3568.

Okabe, N., and Adachi, Y. 1998. 1*H*-Indole-3-propionic Acid**.** *Acta Cryst. C*.54: 386-387.

Ott, J. B., and Boerio-Goates, J. 2000. Chemical thermodynamics: Principles and Applications Calculations from Statistical Thermodynamics, London, San Diego, Calif, Academic Press.

Petersilka, M., Gossmann, U. J., and Gross, E. K. U. 1996. Excitation Energies from Time-Dependent Density-Functional Theory. *Phys. Rev. Lett*. 76: 1212–1215.

Playne, M. J., 1985. Propionic and Butyric Acids. In: Moo-Young, M. (Ed.), Comprehensive Biotechnology, vol. 3. Pergamon, New York.

Politzer, P., and Murray, J. S. 2002. The fundamental nature and role of the electrostatic potential in atoms and molecules Theor. *Chem. Acc*. 108: 134–142.

Runge, E., and Gross, E. K. U. 1984. Density-Functional Theory for Time-Dependent Systems. *Phys. Rev. Lett*. 52: 997–1000.

Sajan, D., Josepha, L., Vijayan, N., and Karabacak, M. 2011. Natural bond orbital analysis, electronic structure, non-linear properties and vibrational spectral analysis of L-histidinium bromide monohydrate: A density functional theory. *Spectrochim. Acta A*. 81: 85–98.

Scrocco, E., Tomasi, J., and Lowdin P. (Ed.). 1978. Advances in Quantum Chemistry, Academic Press, New York.

Seeman, P., and Tallerico, T. 1998. Antipsychotic drugs which elicit little or no Parkinsonism bind more loosely than dopamine to brain D2 receptors, yet occupy high levels of these receptors. *Mol. Psychiatry*. 3 (2): 123–134.

Silverstein, M., Bassler, G. C., and Morill, C. 1981. Spectrometric Identification of Organic Compounds, Wiley, New York.

Silverstein, R. M., Webster, F. X., and Kiemle, D. J. 2005. Spectrometric Identification of Organic Compounds, 7th ed., John Wiley & Sons, New York.

Socrates, G. 2001. Infrared and Raman Characteristic Group Frequencies, Tables and Charts, 3rd ed., John Wiley and Sons Ltd, Chichester.

Sridevi, C., Shanthi, G., and Velraj, G. 2012. Structural, vibrational, electronic, NMR and reactivity analyses of 2-amino-4H-chromene-3-carbonitrile (ACC) by ab initio HF and DFT calculations. *Spectrochim. Acta A*. 89: 46-54.

Surisseau, C., and Marvell, P. 1994. Optical and resonance Raman scattering study of two ‘bisazo’ pigments derived from substituted benzene-2′-azonaphthols. *J. Raman Spectrosc*. 25: 477–788.

Udhayakala, P., Jayanthi, A., Rajendiran, T. V., and Gunasekaran, S. 2011. Computation and interpretation of Vibrational spectra, thermodynamical and HOMO-LUMO analysis of 2-chloro-4-nitroaniline, *Int. J. Chem. Tech.Res*. 3: 1851–1862.

Yildirim, G., Zalaoglu, Y., Kirilmis, C., Koca, M., and Terzioglu, C. 2011. A characterization study on 2,6-dimethyl-4-nitropyridine N-oxide by density functional theory calculations. *Spectrochim. Acta A*. 81: 104–110.

Zhang, R., Dub, B., Sun, G., and Sun, Y. 2010. Experimental and theoretical studies on *o*-, *m*- and *p*-chlorobenzylideneamino antipyrines. *Spectrochim. Acta A*. 75: 1115–1124.

****